

Functional Significance of Wnt Inhibitory Factor-1 Gene in Kidney Cancer

Kazumori Kawakami,¹ Hiroshi Hirata,¹ Soichiro Yamamura,¹ Nobuyuki Kikuno,¹ Sharanjot Saini,¹ Shahana Majid,¹ Yuichiro Tanaka,¹ Ken Kawamoto,² Hideki Enokida,² Masayuki Nakagawa,² and Rajvir Dahiya¹

¹Department of Urology, Veterans Affairs Medical Center and University of California at San Francisco, San Francisco, California and ²Department of Urology, Kagoshima University, Kagoshima, Japan

Abstract

Wnt inhibitory factor-1 (WIF-1) has been identified as one of the secreted antagonists that bind Wnt protein. WIF-1 has been described as a tumor suppressor in various types of cancer. However, the molecular function of WIF-1 gene has never been examined in human renal cell carcinoma (RCC). Therefore, we hypothesized that WIF-1 functions as a tumor suppressor gene and overexpression of this gene may induce apoptosis and inhibit tumor growth in RCC cells. Immunohistochemistry and real-time reverse transcription-PCR revealed that WIF-1 was significantly downregulated in RCC samples and RCC cell lines, respectively. Bisulfite sequencing of the WIF-1 promoter region in RCC cell lines showed it to be densely methylated, whereas there was no methylation of WIF-1 promoter in normal kidney. Significant inhibition of cell growth and colony formation in WIF-1-transfected cells compared with controls were observed. WIF-1 transfection significantly induced apoptosis and suppressed *in vivo* tumor growth. Also, Wnt signaling activity and β -catenin expression were reduced by WIF-1 transfection. In conclusion, this is the first report documenting that the WIF-1 is downregulated by promoter methylation and functions as a tumor suppressor gene by inducing apoptosis in RCC cells. [Cancer Res 2009;69(22):8603–10]

Introduction

Renal cell carcinoma (RCC) accounts for 2% to 3% of human malignancies and is the seventh most frequent cause of tumor-dependent death among men (1). The most common histologic subtypes of sporadic kidney tumors are clear cell RCC (ccRCC; ref. 2).

The wingless-type (Wnt) proteins constitute a 19-member family of secreted glycoproteins that are involved in development and oncogenesis (3). Aberrant expression of Wnt signaling has been reported in various human cancers, including colorectal cancer (4), melanoma (5), non-small cell lung cancer (6), leukemia (7), and bladder cancer (8). Constitutive activation of the Wnt signaling pathway can be induced by deregulation of Wnt pathway members, such as overexpression of β -catenin and disheveled (4, 6). Also, downregulation of endogenous Wnt antagonists can result

in unregulated Wnt signaling (9, 10). Wnt antagonists can be divided into two functional classes, the secreted frizzled-related protein (sFRP) class and the Dickkopf (Dkk) class. Members of the sFRP class, which includes the sFRP family (sFRP-1, sFRP-2, sFRP-3, sFRP-4, and sFRP-5), WIF-1, and Cerberus, bind directly to Wnts, thereby altering their ability to bind to the Wnt receptor complex. Members of the Dkk class, which comprises certain Dkk family proteins (Dkk-1, Dkk-2, Dkk-3, and Dkk-4), inhibit Wnt signaling by binding to the LRP5/LRP6 component of the Wnt receptor complex (11). In normal conditions, β -catenin is controlled by the upstream regulators of the Wnt signaling pathway (12). At the cell surface, the binding of Wnt protein with its frizzled transmembrane receptor activates disheveled phosphoprotein, which, in turn, inactivates glycogen synthase kinase-3 β . The inhibited glycogen synthase kinase-3 β fails to phosphorylate β -catenin, which, in turn, cannot form a complex with adenomatous polyposis coli to form an ubiquitin-mediated proteolytic complex and be degraded. Consequently, β -catenin accumulates in the cytoplasm and enters the nucleus. As a transcriptional activator, β -catenin in the nucleus binds to members of the TCF/LEF family and activates the target genes, including *c-myc* and *cyclin D1* (13, 14). This is a known canonical pathway of Wnt signaling.

Recently, it has become clear that gene function can be altered by epigenetic alterations. Silencing of tumor suppressor genes by hypermethylation of CpG islands within the promoter and/or 5'-regions is a common feature of human cancer and is often associated with partial or complete transcriptional block. Many (candidate) tumor suppressor genes silenced by DNA methylation have been reported for primary RCC cases and/or analyzed in RCC cell lines (15–17).

Wnt inhibitory factor-1 (WIF-1) is highly conserved between species and was initially identified in the human retina (18). The downregulation of WIF-1 by promoter hypermethylation has been reported in various human malignancies including carcinoma of urinary bladder (8), lung (19), breast (20), esophagus (21, 22), and stomach (23). In addition, it has been shown that WIF-1 functions as a tumor suppressor in melanoma (24), nasopharyngeal (22), esophageal (21, 22), stomach (23), breast (25), and lung (26) cancers. With regard to RCC, a previous report from our laboratory showed that the methylation frequency of the Wnt antagonists could serve as biomarkers for RCC (27), but no functional studies of the WIF-1 gene in RCC have been reported.

Therefore, in the present study, we hypothesized that WIF-1 is densely methylated in its promoter region and functions as a tumor suppressor gene in RCC. To address this issue, we checked the mRNA and protein expression levels in RCC cell lines and human RCC tissues, respectively. We also overexpressed WIF-1 by nonviral gene transfer to RCC cells and examined the effect on RCC cells *in vitro* and tumor growth *in vivo* using empty vector (EV)– or

Note: Supplementary data for this article are available at Cancer Research Online (<http://cancerres.aacrjournals.org/>).

Requests for reprints: Rajvir Dahiya, Urology Research Center (112F), Veterans Affairs Medical Center and University of California at San Francisco, 4150 Clement Street, San Francisco, CA 94121. Phone: 415-750-6964; Fax: 415-750-6639; E-mail: rdahiya@urology.ucsf.edu.

©2009 American Association for Cancer Research.

doi:10.1158/0008-5472.CAN-09-2534

WIF-1-transfected cells. In addition, apoptosis was analyzed with EV-transfected and WIF-1-transfected cells and the expression of β -catenin after gene replacement was analyzed.

Materials and Methods

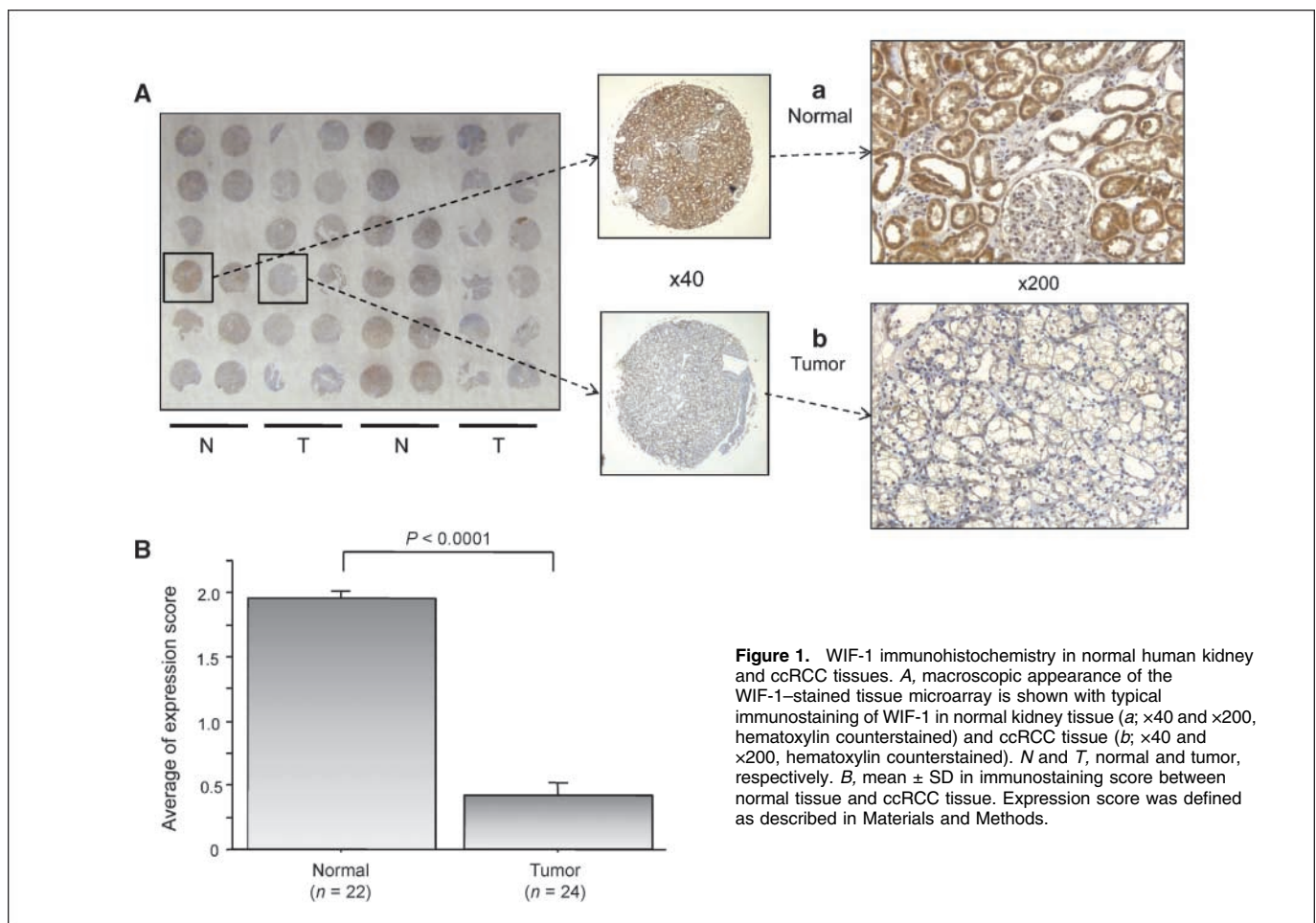
Immunohistochemistry. A tissue microarray that consisted of 24 ccRCC and matched adjacent tissue 1.5 cm away from carcinoma was obtained from US Biomax (KD481). Detailed information on all tumor samples can be found at <http://www.biomax.us/index.php>. Immunostaining was done on the tissue microarray using the UltraVision Detection System (TM-015-HD; Thermo Scientific) following the manufacturer's protocol. Antigen retrieval was carried out by microwaving the slide in 10 mmol/L sodium citrate. The slide was incubated overnight with a 1:100 dilution of anti-WIF-1 antibody (R&D Systems). A pathologist not involved in the present study evaluated the immunostaining under blind conditions. Immunohistochemical staining was graded on an arbitrary scale from 0 to 2: 0 representing negative expression (0-20% positive cells), 1 representing weakly positive expression (20-50% positive cells), and 2 representing strongly positive expression (50-100% positive cells). The scale was determined according to the average number of positive cells in 10 random fields of the slide (17).

Cell culture and 5-aza-2'-deoxycytidine treatment. We used three human kidney cancer cell lines, Caki-2, ACHN, and A498, obtained from the American Type Culture Collection. The Caki-2 and A498 cell lines were incubated in RPMI 1640 supplemented with 10% fetal bovine serum. ACHN cells were maintained in Eagle's MEM supplemented with 10% fetal bovine serum. These cells were incubated in a humidified incubator (5% CO₂) at

37°C. For 5-aza-2'-deoxycytidine (DAC; Sigma-Aldrich) treatment, cells (8×10^5 per 100 mm cell culture dish) were treated with DAC (5 μ mol/L) for 4 days. Culture medium and DAC were replaced daily.

RNA extraction and reverse transcription-PCR. Total RNA was isolated using the RNeasy Mini kit (Qiagen) following the manufacturer's directions. Reverse transcription reactions were carried out with 2 μ g total RNA using a Reverse Transcription System Kit (Promega). Semiquantitative reverse transcription-PCR (RT-PCR) was done using REDTaq (Sigma-Aldrich). The primer sequences and PCR conditions are shown in Supplementary Table S1. Quantitative real-time RT-PCR analysis was done in triplicate with an Applied Biosystems Prism 7500 Fast Sequence Detection System using TaqMan universal PCR master mix according to the manufacturer's specifications (Applied Biosystems). The TaqMan primer IDs purchased from Applied Biosystems are as follows: WIF-1, Hs00183662_m1; β -catenin, Hs00355045_m1; and glyceraldehyde-3-phosphate dehydrogenase, Hs99999905_m1. The human glyceraldehyde-3-phosphate dehydrogenase gene was used as an endogenous control. The thermal cycler conditions were as follows: hold for 20 s at 95°C followed by two-step PCR for 40 cycles of 95°C for 3 s followed by 60°C for 30 s. Levels of RNA expression were determined using the 7500 Fast System SDS software version 1.3.1 (Applied Biosystems).

DNA extraction and bisulfite DNA sequencing. Genomic DNA was extracted from RCC cells with a QIAamp DNA mini kit (Qiagen) following the manufacturer's protocol. Bisulfite modification of genomic DNA was done using the EpiTect Bisulfite kit (Qiagen) following the manufacturer's directions. The genomic DNA from adult human normal kidney tissue (BioChain) was also modified and used as a control. Primers for bisulfite genomic sequencing PCR were designed by using the online program



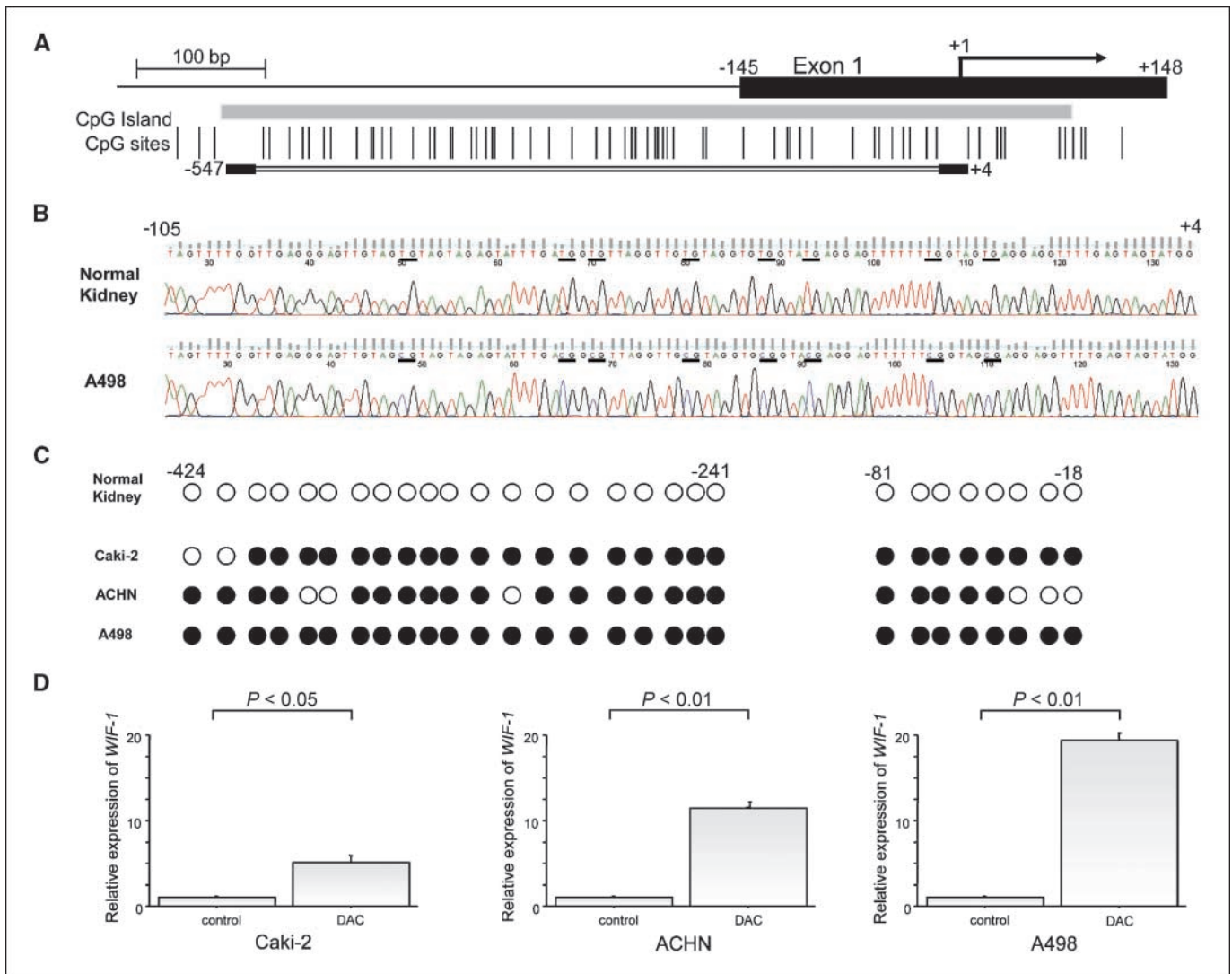


Figure 2. Methylation of the human WIF-1 gene promoter. *A*, schematic representation of the promoter region of the human WIF-1 gene and primer location. *Vertical lines*, location of CpG dinucleotides; *gray box*, CpG island; *black box*, first exon; *arrows*, approximate position of the transcription start site; *doubled horizontal line*, region examined by bisulfite DNA sequencing. *B*, representative results of the bisulfite sequencing for the normal kidney and the A498 cells (from -105 to +4). The horizontal bars and the ATG surrounded with black boxes indicate CpG sites and the start codon, respectively. *C*, methylation mapping of 28 CpG sites of the WIF-1 promoter region obtained from bisulfite sequencing in normal kidney and RCC cell lines (from -424 to -241 and from -105 to +4). *White and black circles*, unmethylated and methylated CpG sites, respectively. *D*, upregulation of WIF-1 mRNA expression following treatment with DAC in RCC cell lines. Levels of WIF-1 mRNA expression were quantified by real-time RT-PCR.

MethPrimer (28) or by referring to previous reports (8, 19). The primer sequences and PCR conditions are shown in Supplementary Table S1. The fragment amplified corresponded to the WIF-1 promoter region -547 to +4 (the ATG start codon of WIF-1 was defined as +1). The detailed procedure for PCR was described previously (17). The amplification products were confirmed by electrophoresis on a 2% agarose gel and sequenced directly by an outside vendor (McLab).

Transfection and colony formation assay. A human WIF-1 expression vector (pcDNA-WIF-1) was constructed by subcloning the full-length cDNA of WIF-1 (Invitrogen) with a FLAG epitope-tagged sequence into *HindIII-XhoI* sites of pcDNA3.1(+) vector (Invitrogen). Caki-2, ACHN, and A498 cells (1×10^5 per well of 6-well plate) were transfected with pcDNA-WIF-1 or with pcDNA3.1(+) vector (EV) using FuGENE HD (Roche Applied Science) according to the manufacturer's protocol. The transfected A498 cells were transferred to 10 cm cell culture dishes and selected with 400 $\mu\text{g}/\text{mL}$ G418 (Invitrogen). Colonies were stained with 0.5% methylene blue 3 weeks after transfection and data were obtained from three independent experiments.

Cell lines stably expressing FLAG-WIF-1 were maintained with 200 $\mu\text{g}/\text{mL}$ G418.

WIF-1 knockdown by small interfering RNA. Stable cells (A498-WIF-1) were transfected with WIF-1 small interfering RNA (1299003; Invitrogen) or negative control (Invitrogen) using Lipofectamine 2000 (Invitrogen) following the manufacturer's protocol. The mRNA expression was checked by quantitative and semiquantitative RT-PCR 72 h after transfection.

Cell proliferation assay. For cell proliferation assay, Caki-2, ACHN, and A498 cells were seeded in 96-well microplates at a density of 5×10^3 per well 24 h before transfection. After transient transfection with EV or WIF-1, cells were incubated for 144 h and cell viability was determined every 24 h by using the CellTiter 96 Aqueous One Solution Cell Proliferation Assay kit (Promega) according to the manufacturer's protocol. Absorbance at 490 nm was measured with a kinetic microplate reader (Spectra MAX 190; Molecular Devices) and used as a measure of cell number. Experiments were done in quadruplicate and repeated three times. Cell proliferation assays with WIF-1 small interfering RNA were done for 72 h using the same

method. For assay of stable transfectants, EV-transfected or WIF-1-transfected A498 cells were seeded at a density of 1×10^3 per well in 96-well microplates and incubated for 120 h. Cell viability was checked every 24 h as described above.

Apoptosis analysis. A498 cells transiently transfected with EV or WIF-1 were harvested 72 h after transfection by trypsinization and stained using an Annexin V-FITC/7-AAD KIT (Beckman Coulter) according to the manufacturer's protocol and immediately analyzed by flow cytometry (Cell Lab Quanta SC; Beckman Coulter). Experiments were done in duplicate and repeated independently three times.

Tumor growth in nude mice. All *in vivo* experiments were done with approval by the Animal Studies Subcommittee of the VAMC (protocol no. 08-003-01). Groups of six female nude mice (strain BALB/c *nu/nu*; Charles River Laboratories), 4 to 5 weeks old, received s.c. injections of A498-EV or A498-WIF-1 cells (1×10^7 in 200 μ L) in the right flank area. Tumor size was determined with calipers once per week for 7 weeks, and tumor volume was calculated based on width (x) and length (y): $x^2y/2$, where $x < y$. After the mice were killed, tumors were resected and weighted. Tumor tissues were fixed in 10% formalin, embedded in paraffin, and stained with anti-WIF-1 antibody using the same method as described above.

Analysis of Wnt signaling activity. A498 cells (2×10^3 per well) were plated in 96-well plates at 24 h before transfection. A498 cells were transiently cotransfected with the TCF/LEF reporter plasmid (SABiosciences) and EV or WIF-1 according to the protocol of the manufacturer. Luciferase assays were carried out using the Dual-Luciferase Reporter Assay System

(Promega) according to the manufacturer's protocol. Light emission was quantified with a TD-20/20 luminometer (Turner Biosystems). Experiments were done in triplicate and signals were normalized for transfection efficiency to the internal *Renilla* control.

Western analysis. Protein extraction was done with radioimmunoprecipitation assay buffer (Thermo Scientific) and the extracts (20 μ g) were separated on 4% to 20% polyacrylamide gels (Thermo Scientific) and transferred to polyvinylidene fluoride (Hybond-P; GE Healthcare) membranes by electroblotting using Trans-Blot SD Semi-Dry Transfer Cell (Bio-Rad). The membranes were blocked with 0.3% skim milk at room temperature for 1 h. Subsequently, the membranes were incubated with antibody against FLAG (Sigma-Aldrich), β -catenin (Cell Signaling), or glyceraldehyde-3-phosphate dehydrogenase (Cell Signaling) overnight. After washing, the membranes were incubated with horseradish peroxidase-linked secondary antibodies (GE Healthcare) at room temperature for 1 h. The proteins were visualized using the ECL detection system (GE Healthcare).

Statistical analysis. Data are shown as mean \pm SD. The Student's *t* test was used to compare the two different groups. *P* values < 0.05 were regarded as statistically significant. All statistical analyses were done using StatView version 5.0 for Windows.

Results

Immunostaining of WIF-1 in normal human kidney and kidney cancer specimens. To examine the expression levels of WIF-1

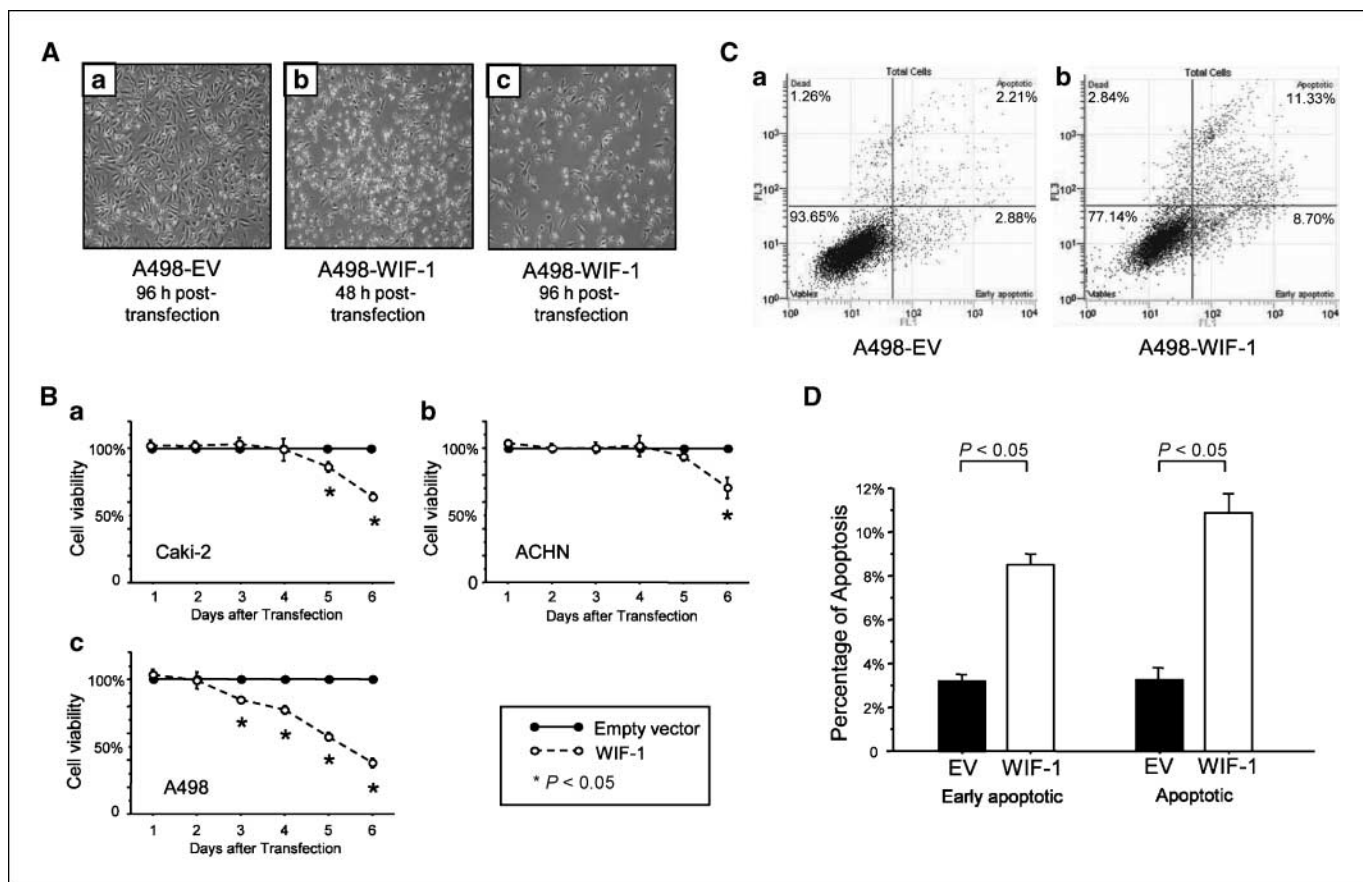


Figure 3. Characteristics of WIF-1-transfected RCC cells. *A*, effect of WIF-1 transfection on the morphology of A498 cells. Photographs ($\times 100$) of EV-transfected A498 cells at 96 h after transient transfection (*a*) and WIF-1-transfected A498 cells at 48 h (*b*) and 96 h (*c*) after transfection are shown. *B*, effect of WIF-1 transfection on the viability of Caki-2 (*a*), ACHN (*b*), and A498 (*c*) cell lines in cell proliferation assay. WIF-1-transfected cell viability was calculated assuming that EV-transfected cell viability was 100% at each time point. *C*, effect of WIF-1 transfection on apoptosis in A498 cells. Annexin V-FITC/7-AAD staining discriminates between cells in early (*bottom right quadrant*) and advanced (*top right quadrant*) apoptotic states. Viable cells are double negative (*bottom left quadrant*). The representative apoptotic cell fractions in EV-transfected or WIF-1-transfected A498 cells are shown as *a* or *b*, respectively. *D*, proportion of early apoptotic and apoptotic cells. Data are expressed as the percentage of early apoptotic and apoptotic cells out of the total measured cell population of A498 cells.

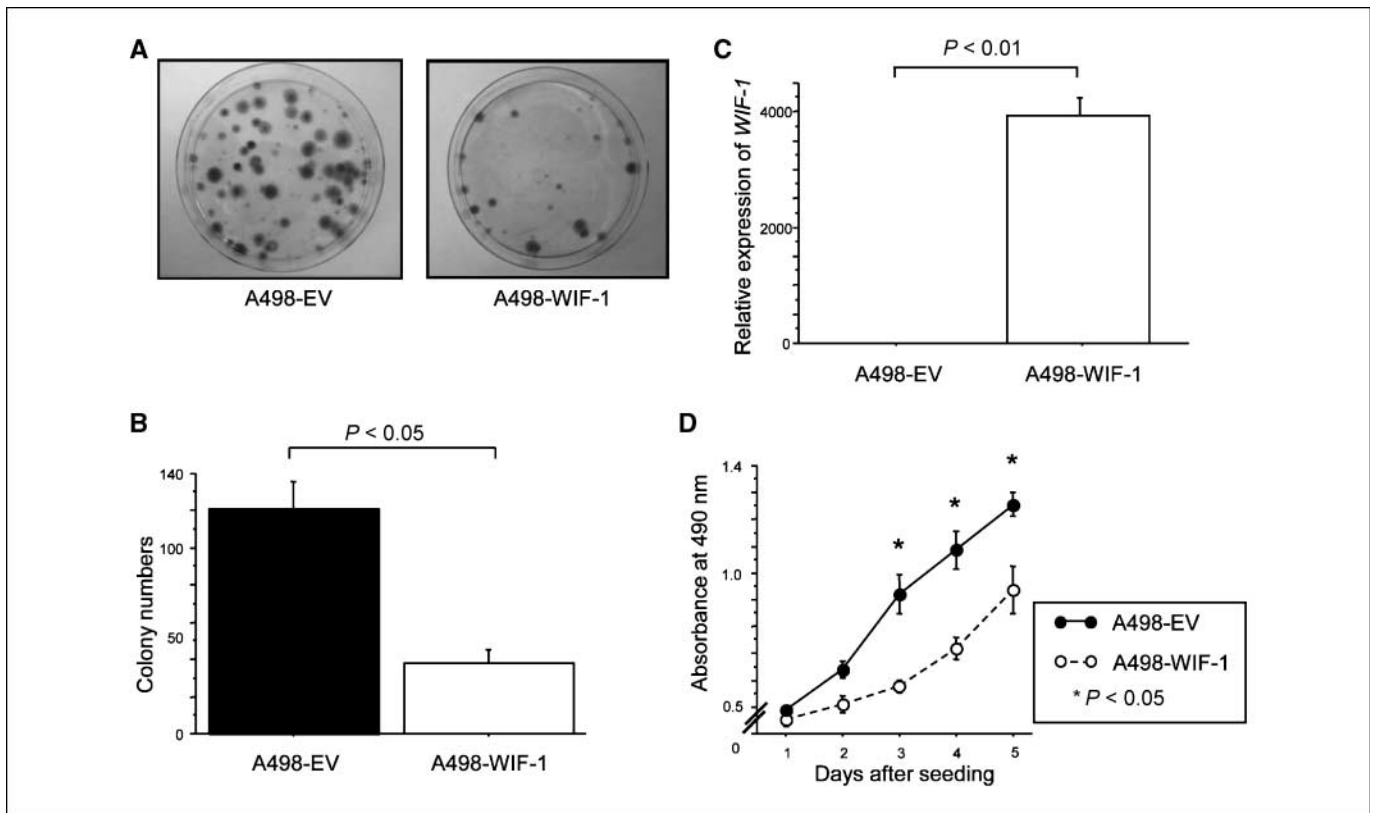


Figure 4. Colony formation assay and cell proliferation assay of stably transfected WIF-1 cells. *A*, representative photograph of colony formation assay. Photographs of the stained colonies in 10 cm dishes for EV (*left*) and WIF-1 (*right*) after selection with G418 (400 μ g/mL) are shown. *B*, quantitative analyses of the results in *A*. Mean \pm SD of three independent experiments. *C*, WIF-1 gene expression in stable A498 cells transfected with EV or WIF-1. The result of real-time RT-PCR is shown. *D*, result of cell proliferation assay for stable cell lines. Black or white circles, absorbance at 490 nm of EV-transfected or WIF-1-transfected cells, respectively.

in malignant and normal kidney tissues, immunostaining was done on a tissue microarray using antibody to WIF-1. The macroscopic appearance of the tissue microarray and typical immunostaining of WIF-1 in normal (*a*) and ccRCC (*b*) specimens ($\times 40$ and $\times 200$) are shown in Fig. 1A. The staining was much stronger in normal specimens than in ccRCC. The mean expression score (1.955 ± 0.213) in normal specimens ($n = 22$) was significantly higher compared with that (0.417 ± 0.504) in ccRCC specimens ($n = 24$; $P < 0.0001$; Fig. 1B).

Methylation status of the WIF-1 promoter region and restoration of WIF-1 mRNA expression in RCC cells after DAC treatment. The methylation status at 28 CpG sites of the WIF-1 CpG island was characterized in three RCC cell lines and normal kidney DNA by bisulfite genomic sequencing (Fig. 2A-C). These analyses indicated that the CpG island in each cell line showed essentially the same methylation status. The promoter regions checked in this study of these three RCC cell lines were densely methylated, whereas the same region of normal kidney was unmethylated. In addition, we confirmed that WIF-1 expression in RCC cells was significantly restored after treatment with the demethylating agent, DAC ($P < 0.05$ for Caki-2 and $P < 0.01$ for ACHN and A498, respectively; Fig. 1D).

Suppression of RCC cell growth by WIF-1 transfection. To evaluate the effect of WIF-1 restoration on RCC cell growth, we transfected cells with a WIF-1-expressing pcDNA3.1(+) vector (WIF-1). WIF-1 transcription was significantly increased at 72 h after transfection with WIF-1 but not in untreated cells or those treated with empty pcDNA3.1(+) vector (EV; $P < 0.01$ for all three

cell lines; Supplementary Fig. S1A and B). The increase in WIF-1 transcription was highest in A498 cells. To examine the role of WIF-1 in RCC cell proliferation, we checked the effect of WIF-1 transfection on RCC cell viability. As shown in Fig. 3A, WIF-1 transfection decreased A498 cell viability compared with those transfected with EV. WIF-1-transfected cells were sparse and less dense than EV-transfected cells 48 and 96 h after transfection. We checked the expression levels of WIF-1 by quantitative real-time RT-PCR at 48 and 96 h after transfection in A498 cells (data not shown) and found that the expression levels were also significantly higher and almost similar to that at 72 h after transfection compared with that of EV-transfected cells (Supplementary Fig. S1A and B). Growth inhibition by WIF-1 transfection was also confirmed by cell proliferation assays on all three RCC cell lines. WIF-1 transfection significantly decreased RCC cell viability in a time-dependent manner ($P < 0.05$; Fig. 3B).

Promotion of apoptosis and suppression of colony formation efficiencies in RCC cells by WIF-1 transfection. We also evaluated apoptosis by using flow cytometry with A498 cells that were transiently transfected with EV or WIF-1. As shown in Fig. 3C, the apoptotic cell fractions (early apoptotic + apoptotic) were 5.09% in EV-transfected A498 cells and 20.03% in those transfected with WIF-1. Thus, WIF-1 transfection significantly induced apoptosis in A498 cells ($P < 0.05$ for both early apoptotic and apoptotic; Fig. 3D). In stably transfected A498 cells, the colony formation efficiency was significantly suppressed after transfection with WIF-1 compared with that observed in EV-transfected cells ($P < 0.05$; Fig. 4A and B).

In vivo and in vitro growth using stably transfected WIF-1 cells. We made A498 stable cell lines transfected with either EV (A498-EV) or WIF-1 gene (A498-WIF-1). A498-WIF-1 cells expressed high levels of WIF-1 and showed significant inhibition of growth compared with A498-EV cells ($P < 0.01$; Fig. 4C and $P < 0.05$ for days 3-5; Fig. 4D, respectively). These cells were also used in an *in vivo* study using nude mice. The macroscopic appearance of tumor at day 50 after inoculation showed a larger mass in A498-EV mouse xenografts than that in A498-WIF-1 xenografts (Fig. 5A). The average volume and weight of tumors were significantly reduced in mice injected with A498-WIF-1 cells (Fig. 5B and C, respectively). Histologic findings from H&E staining confirmed that both xenografted tumors consisted of viable cancer cells with solid proliferation and no significant change of appearance was observed (data not shown). After 50 days, WIF-1 expression in A498-WIF-1-inoculated tumors was higher than that of A498-EV-inoculated tumors by immunohistochemistry (Fig. 5D). There was no statistically significant difference in the body weight of the mice, nor did there appear to be any obvious toxicity from the injection (data not shown).

Effect of WIF-1 knockdown on cell growth. To further confirm that WIF-1 functions as a tumor suppressor, WIF-1 expression in A498-WIF-1 stable cells was knocked down by RNA

interference and cell proliferation assays were done. Knockdown of WIF-1 expression was verified by both quantitative and semiquantitative RT-PCR ($P < 0.01$; Supplementary Fig. S2A). After WIF-1 knockdown, cell proliferation was significantly increased compared with that of cells transfected with negative control ($P < 0.05$ at 3 days after transfection; Supplementary Fig. S2B).

Downregulation of Wnt signaling activity and β -catenin expression by WIF-1 transfection. To determine the effect of WIF-1 transfection on Wnt signaling activity, we performed luciferase assays and Western blotting analysis in A498 cells transiently cotransfected with WIF-1 or EV and a TCF/LEF reporter plasmid. Luciferase assays showed a significant reduction in TCF-dependent transcriptional activity in A498 cells transfected with WIF-1 compared with that in EV-transfected cells ($P < 0.05$; Fig. 6A). We subsequently checked β -catenin expression in EV-transfected and WIF-1-transfected A498 cells by real-time RT-PCR and Western blotting because β -catenin is a key molecule in the Wnt signaling pathway. β -Catenin was significantly downregulated in WIF-1-transfected cells compared with EV-transfected cells in real-time RT-PCR ($P < 0.01$; Fig. 6B) and Western blot analysis (Fig. 6C).

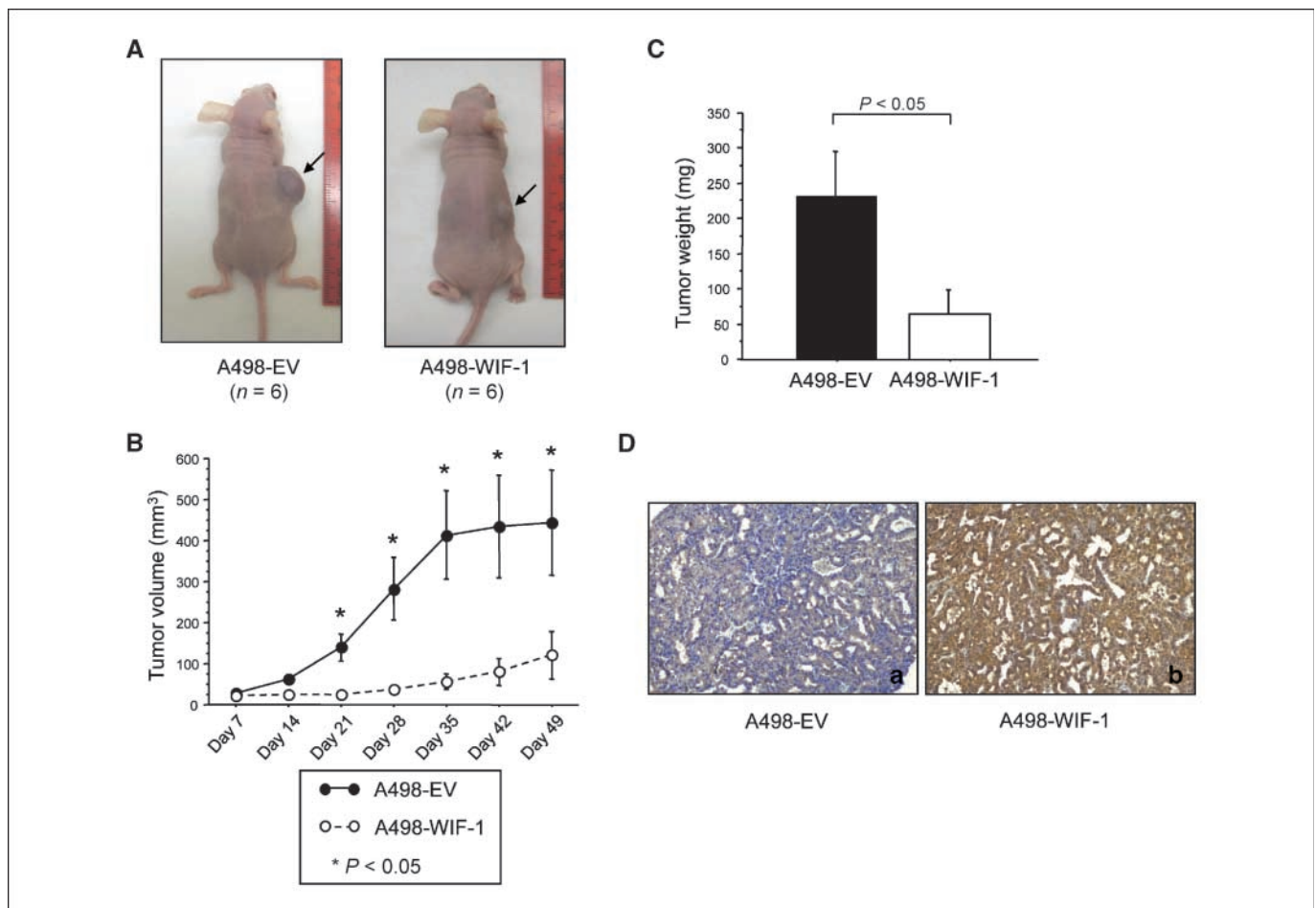


Figure 5. *In vivo* tumor growth of WIF-1-transfected A498 cells. **A**, macroscopic appearance of the tumors on day 50 after s.c. inoculation of A498-EV (left) and A498-WIF-1 (right) cells. **B**, tumor growth curves in nude mice. Black or white circles, mean \pm SD of tumor volume (mm³) for EV-transfected or WIF-1-xenografted mice, respectively. **C**, mean \pm SD of tumor weight on day 50. **D**, representative photographs (x100) of WIF-1 staining of each group (a, EV-inoculated mouse; b, WIF-1-inoculated mouse).

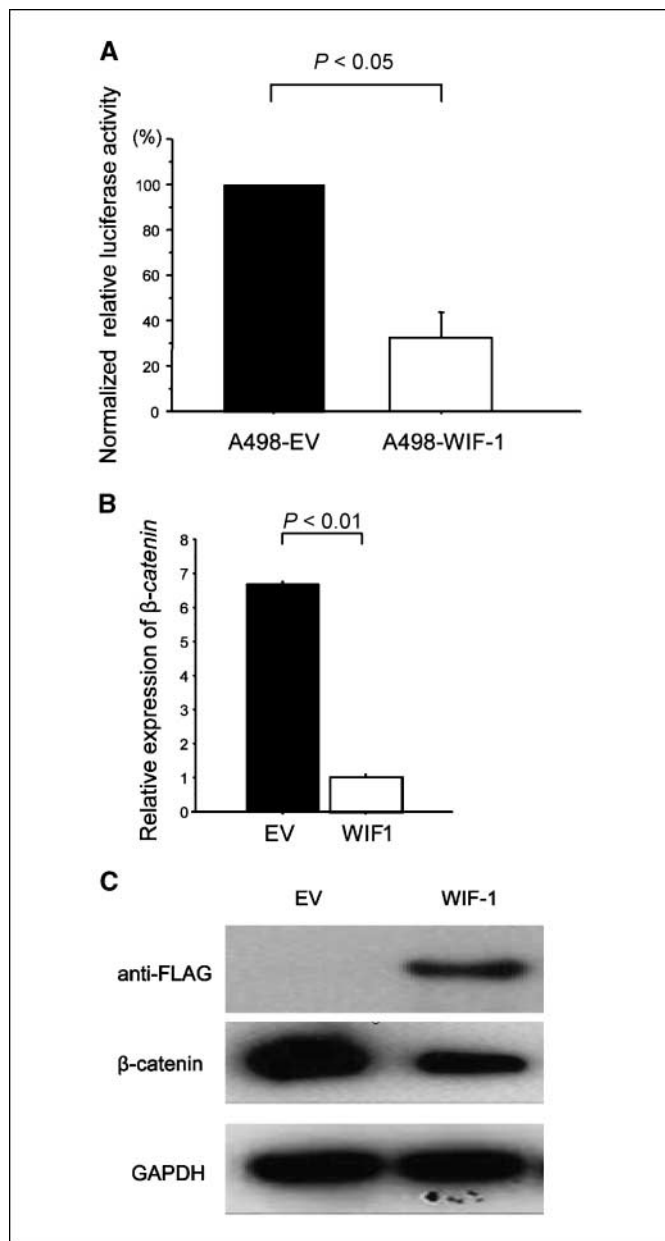


Figure 6. Effect of the restoration of WIF-1 expression on Wnt signaling and β -catenin expression. *A*, effect on the Wnt-dependent transcription activity. Black or white columns, relative luciferase activity of EV-transfected or WIF-1-transfected A498 cells, respectively, which were both cotransfected with the TCF/LEF reporter plasmid. *B*, real-time RT-PCR for β -catenin. *C*, Western blotting for FLAG and β -catenin. Typical immunoblotting results of FLAG, β -catenin, and glyceraldehyde-3-phosphate dehydrogenase (GAPDH) protein levels in EV-transfected or WIF-1-transfected A498 cells are shown.

Discussion

The WIF-1 gene has been recently identified as a secreted protein that binds to Wnt proteins and inhibits their interaction with the frizzled receptor; this leads to the termination of transcription of genes activated by the β -catenin/TCF/LEF transcriptional complex (18). Thus, it is possible that functional loss of WIF-1 results in activation of the Wnt signaling pathway, with increased proliferation and uncontrolled differentiation leading to carcinogenesis. To date, decreased WIF-1 mRNA and protein expression has been ob-

served in several cancers (8, 19–26, 29). Recently, Urakami and colleagues (27) carried out methylation analyses of six Wnt antagonist family genes (sFRP-1, sFRP-2, sFRP-4, sFRP-5, WIF-1, and Dkk-3) in RCC analyzed by methylation-specific PCR. In their study, all Wnt antagonist genes had significantly higher methylation frequencies in RCC compared with matched normal renal tissue. With regard to sFRP-1, Gumz and colleagues (30) reported that restoration of sFRP-1 expression in RCC cells attenuated the tumor phenotype and concluded that sFRP-1 functioned as a tumor suppressor. However, the molecular function of other Wnt antagonist genes, including WIF-1, remains unknown in human RCC. Therefore, in the present study, we examined whether WIF-1 functions as a tumor suppressor in RCC cells.

We found for the first time that WIF-1 is significantly down-regulated at the protein level in the tissue microarray of human ccRCC specimens and at the mRNA level in RCC cell lines. Bisulfite sequencing of the WIF-1 promoter region showed it to be densely methylated in RCC cell lines, whereas there was no methylation in the normal kidney DNA. In addition, treatment with demethylation agent (DAC) significantly restored WIF-1 mRNA expression in RCC cell lines. These results are consistent with studies in other types of cancer such as bladder, lung, breast, esophagus, and stomach cancers (8, 19–23). Our results also indicate that downregulation of WIF-1 expression in RCC cell lines and human cancer tissues correlate with CpG methylation of the WIF-1 promoter. Using RCC cell lines transfected with a WIF-1 expression plasmid, we also showed for the first time that reexpression of WIF-1 significantly inhibited cell growth in all three RCC cell lines tested. Conversely, when WIF-1 expression was subsequently knocked down by RNA interference, cell proliferation was increased. These results strongly indicate that WIF-1 functions as a tumor suppressor in RCC cells. Urakami and colleagues (8) also showed that the knockdown of the WIF-1 gene in a human bladder cell line (UMUC) that expresses relatively high levels of WIF-1 resulted in increased cell growth. Furthermore, we have also found that WIF-1 restoration significantly induces apoptosis in RCC cells. Targeted inhibition of Wnt signaling by WIF-1 transfection has been shown to inhibit cell growth in other cancers (21–26). For instance, Kim and colleagues (26) reported that recombinant human WIF-1 significantly inhibited lung cancer cell growth and WIF-1 transfection significantly increased apoptotic cell death. Moreover, Ohigashi and colleagues (31) showed that overexpression of WIF-1 resulted in sensitizing PC-3 prostate cancer cells for paclitaxel to induce apoptosis. In contrast, Gumz and colleagues (30) reported that restoration of sFRP-1 significantly inhibited cell proliferation of UMRC3 RCC cells but did not promote apoptosis. Positive Wnt signaling has been reported to have anti-apoptotic activity in several cell types (31–33) and our results and others suggest that WIF-1 restoration leads to increased apoptosis in several types of cancer.

Other *in vivo* studies on WIF-1 gene have been reported with melanoma and lung cancer (24, 26). In those studies, WIF-1 vector along with transfection agent was injected directly into existing tumor in nude mice. These results were similar to ours in that tumors receiving WIF-1 remained smaller, whereas tumors receiving EV grew in size. In this study, we injected cells stably transfected with either EV (A498-EV) or WIF-1 (A498-WIF-1) that showed significant differences in WIF-1 mRNA expression and growth inhibition *in vitro*. We found that the WIF-1-transfected xenografts showed significant growth inhibition *in vivo*, indicating that WIF-1 acts as a tumor suppressor in RCC cells.

Reduced Wnt signaling activity by WIF-1 restoration has been reported in other studies (8, 21–26, 31). Among them, luciferase assay was done in five studies (21, 23–25, 31) and all showed downregulation of Wnt signaling activity. Others showed inhibition of Wnt signaling by validating the downregulation of β -catenin expression at the mRNA and/or protein levels. Similarly, we found downregulation of Wnt signaling activity and downregulation of β -catenin expression at both mRNA and protein levels, which are consistent with these previous reports.

In conclusion, we have shown for the first time that WIF-1 is frequently downregulated in RCC cell lines and clinical ccRCC tissues. WIF-1 restoration caused suppression of RCC cell growth *in vitro* and tumor growth *in vivo*. In addition, WIF-1 transfection induced apoptosis and reduced Wnt signaling activity in RCC cells. These results suggest that WIF-1 functions as a tumor suppressor

gene in RCC cells and that restoration of WIF-1 might offer a new therapeutic approach for the treatment of RCC patients.

Disclosure of Potential Conflicts of Interest

No potential conflicts of interest were disclosed.

Acknowledgments

Received 7/7/09; revised 8/27/09; accepted 9/12/09; published OnlineFirst 11/3/09.

Grant support: NIH grants RO1CA130860, RO1CA111470, and T32DK007790; VA REAP award; and Merit Review grants (Principal Investigator: R. Dahiya).

The costs of publication of this article were defrayed in part by the payment of page charges. This article must therefore be hereby marked *advertisement* in accordance with 18 U.S.C. Section 1734 solely to indicate this fact.

We thank Dr. Roger Erickson for support and assistance with the preparation of the article.

References

- Jemal A, Murray T, Ward E, et al. Cancer statistics, 2005. *CA Cancer J Clin* 2005;55:10–30.
- Thoenes W, Störkel S, Rumpelt HJ. Histopathology and classification of renal cell tumors (adenomas, oncocytomas and carcinomas). The basic cytological and histopathological elements and their use for diagnostics. *Pathol Res Pract* 1986;181:125–43.
- Polakis P. Wnt signaling and cancer. *Genes Dev* 2000;14:1837–51.
- Morin PJ, Sparks AB, Korinek V, et al. Activation of β -catenin-Tcf signaling in colon cancer by mutations in β -catenin or APC. *Science* 1997;275:1787–90.
- Weeraratna AT, Jiang Y, Hostetter G, et al. Wnt5a signaling directly affects cell motility and invasion of metastatic melanoma. *Cancer Cell* 2002;1:279–88.
- Uematsu K, He B, You L, et al. Activation of the Wnt pathway in non small cell lung cancer: evidence of dishevelled overexpression. *Oncogene* 2003;22:7218–21.
- Lu D, Zhao Y, Tawatao R, et al. Activation of the Wnt signaling pathway in chronic lymphocytic leukemia. *Proc Natl Acad Sci U S A* 2004;101:3118–23.
- Urakami S, Shiina H, Enokida H, et al. Epigenetic inactivation of Wnt inhibitory factor-1 plays an important role in bladder cancer through aberrant canonical Wnt/ β -catenin signaling pathway. *Clin Cancer Res* 2006;12:383–91.
- Rubin JS, Barshishat-Kupper M, Feroze-Merzoug F, et al. Secreted WNT antagonists as tumor suppressors: pro and con. *Front Biosci* 2006;11:2093–105.
- Rubin JS, Bottaro DP. Loss of secreted frizzled-related protein-1 expression in renal cell carcinoma reveals a critical tumor suppressor function. *Clin Cancer Res* 2007;13:4660–3.
- Kawano Y, Kypta R. Secreted antagonists of the Wnt signalling pathway. *J Cell Sci* 2003;116:2627–34.
- Biens M, Clevers H. Linking colorectal cancer to Wnt signaling. *Cell* 2000;103:311–20.
- He TC, Sparks AB, Rago C, et al. Identification of c-MYC as a target of the APC pathway. *Science* 1998;281:1509–12.
- Tetsu O, McCormick F. β -Catenin regulates expression of cyclin D1 in colon carcinoma cells. *Nature* 1999;398:422–6.
- Baldewijns MM, van Vlodrop IJ, Schouten LJ, et al. Genetics and epigenetics of renal cell cancer. *Biochim Biophys Acta* 2008;1785:133–55.
- Esteller M. CpG island hypermethylation and tumor suppressor genes: a booming present, a brighter future. *Oncogene* 2002;21:5427–40.
- Kawamoto K, Hirata H, Kikuno N, et al. DNA methylation and histone modifications cause silencing of Wnt antagonist gene in human renal cell carcinoma cell lines. *Int J Cancer* 2008;123:535–42.
- Hsieh JC, Kodjabachian L, Rebbert ML, et al. A new secreted protein that binds to Wnt proteins and inhibits their activities. *Nature* 1999;398:431–6.
- Mazieres J, He B, You L, et al. Wnt inhibitory factor-1 is silenced by promoter hypermethylation in human lung cancer. *Cancer Res* 2004;64:4717–20.
- Ai L, Tao Q, Zhong S, et al. Inactivation of Wnt inhibitory factor-1 (WIF1) expression by epigenetic silencing is a common event in breast cancer. *Carcinogenesis* 2006;27:1341–8.
- Clément G, Guilleret I, He B, et al. Epigenetic alteration of the Wnt inhibitory factor-1 promoter occurs early in the carcinogenesis of Barrett's esophagus. *Cancer Sci* 2008;99:46–53.
- Chan SL, Cui Y, van Hasselt A, et al. The tumor suppressor Wnt inhibitory factor 1 is frequently methylated in nasopharyngeal and esophageal carcinomas. *Lab Invest* 2007;87:644–50.
- Taniguchi H, Yamamoto H, Hirata T, et al. Frequent epigenetic inactivation of Wnt inhibitory factor-1 in human gastrointestinal cancers. *Oncogene* 2005;24:7946–52.
- Lin YC, You L, Xu Z, et al. Wnt inhibitory factor-1 gene transfer inhibits melanoma cell growth. *Hum Gene Ther* 2007;18:379–86.
- Liu J, Lam JB, Chow KH, et al. Adiponectin stimulates Wnt inhibitory factor-1 expression through epigenetic regulations involving the transcription factor specificity protein 1. *Carcinogenesis* 2008;29:2195–202.
- Kim J, You L, Xu Z, et al. Wnt inhibitory factor inhibits lung cancer cell growth. *J Thorac Cardiovasc Surg* 2007;133:733–7.
- Urakami S, Shiina H, Enokida H, et al. Wnt antagonist family genes as biomarkers for diagnosis, staging, and prognosis of renal cell carcinoma using tumor and serum DNA. *Clin Cancer Res* 2006;12:6989–97.
- Li LC, Dahiya R. MethPrimer: designing primers for methylation PCRs. *Bioinformatics* 2002;18:1427–31.
- Wissmann C, Wild PJ, Kaiser S, et al. WIF1, a component of the Wnt pathway, is down-regulated in prostate, breast, lung, and bladder cancer. *J Pathol* 2003;201:204–12.
- Gumz ML, Zou H, Kreinest PA, et al. Secreted frizzled-related protein 1 loss contributes to tumor phenotype of clear cell renal cell carcinoma. *Clin Cancer Res* 2007;13:4740–9.
- Ohgashi T, Mizuno R, Nakashima J, et al. Inhibition of Wnt signaling downregulates Akt activity and induces chemosensitivity in PTEN-mutated prostate cancer cells. *Prostate* 2005;62:61–8.
- Dehner M, Hadjihannas M, Weiske J, et al. Wnt signaling inhibits Forkhead box O3a-induced transcription and apoptosis through up-regulation of serum- and glucocorticoid-inducible kinase 1. *J Biol Chem* 2008;283:19201–10.
- Tapia JC, Torres VA, Rodriguez DA, et al. Casein kinase 2 (CK2) increases survivin expression via enhanced β -catenin-T cell factor/lymphoid enhancer binding factor-dependent transcription. *Proc Natl Acad Sci U S A* 2006;103:15079–84.

Cancer Research

The Journal of Cancer Research (1916–1930) | The American Journal of Cancer (1931–1940)

Functional Significance of Wnt Inhibitory Factor-1 Gene in Kidney Cancer

Kazumori Kawakami, Hiroshi Hirata, Soichiro Yamamura, et al.

Cancer Res 2009;69:8603-8610. Published OnlineFirst November 3, 2009.

Updated version	Access the most recent version of this article at: doi: 10.1158/0008-5472.CAN-09-2534
Supplementary Material	Access the most recent supplemental material at: http://cancerres.aacrjournals.org/content/suppl/2009/11/03/0008-5472.CAN-09-2534.DC1

Cited articles	This article cites 33 articles, 12 of which you can access for free at: http://cancerres.aacrjournals.org/content/69/22/8603.full#ref-list-1
Citing articles	This article has been cited by 2 HighWire-hosted articles. Access the articles at: http://cancerres.aacrjournals.org/content/69/22/8603.full#related-urls

E-mail alerts	Sign up to receive free email-alerts related to this article or journal.
Reprints and Subscriptions	To order reprints of this article or to subscribe to the journal, contact the AACR Publications Department at pubs@aacr.org .
Permissions	To request permission to re-use all or part of this article, use this link http://cancerres.aacrjournals.org/content/69/22/8603 . Click on "Request Permissions" which will take you to the Copyright Clearance Center's (CCC) Rightslink site.